Dalton Transactions (Revised)

Manuscript ID: DT-ART-08-2012-031774

Electronic Supplementary Information

Mononuclear and dinuclear Re(I) complexes incoporating 1-(2-pyridylazo)-2-naphthol: synthesis, structure, spectral, DFT and TDDFT study†

Pallab Mondal, Amar Hens, Sucharita Basak, and Kajal Krishna Rajak*

Inorganic Chemistry Section, Department of Chemistry, Jadavpur University, Kolkata, 700 032, India

* To whom correspondence should be addressed. Email: kajalrajak@hotmail.com

Jadavpur University

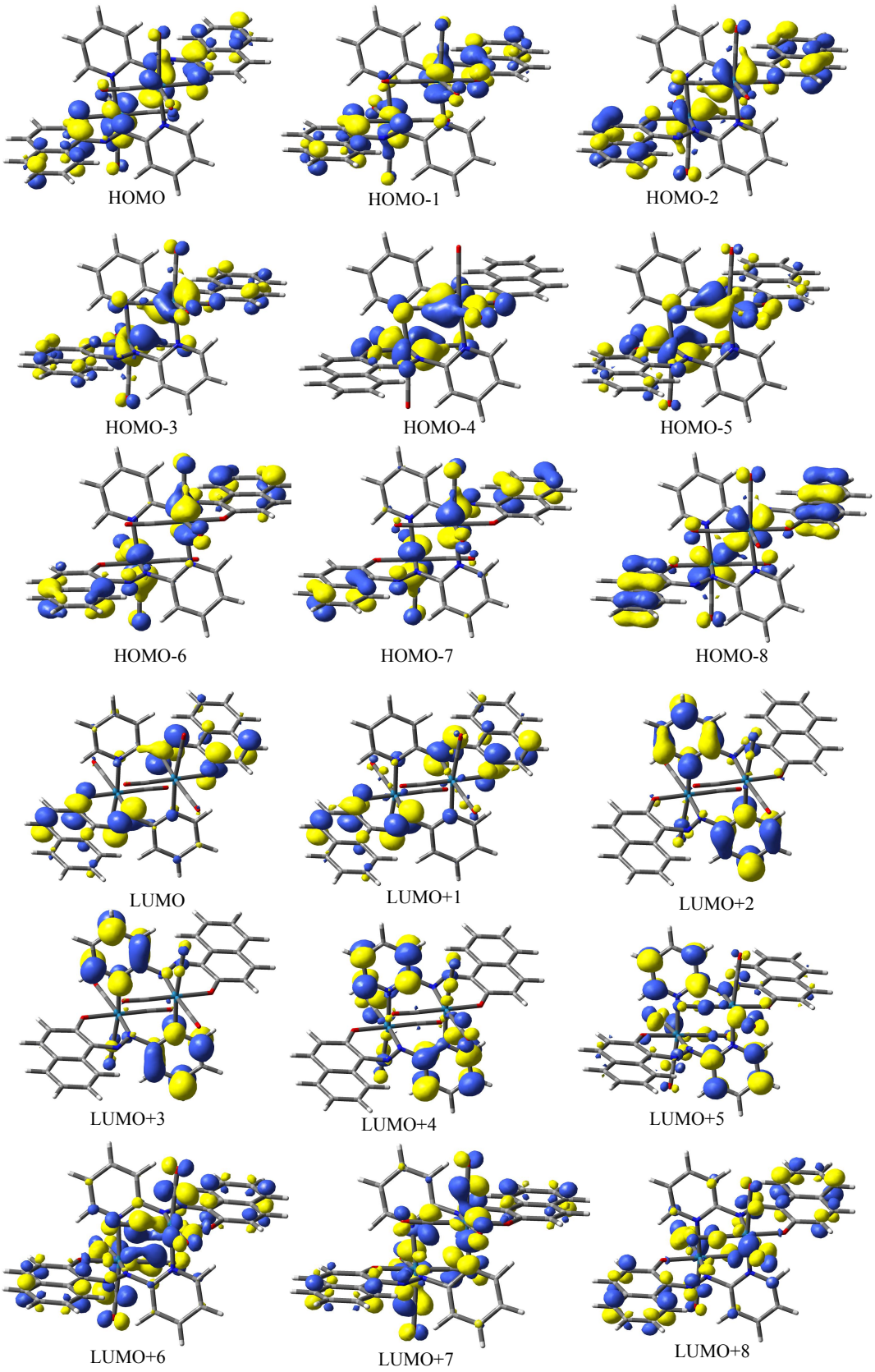

Fig. S1 Isodensity plot of frontier orbitals of $[Re_2(PAN)_2(CO)_6]$, **2**.

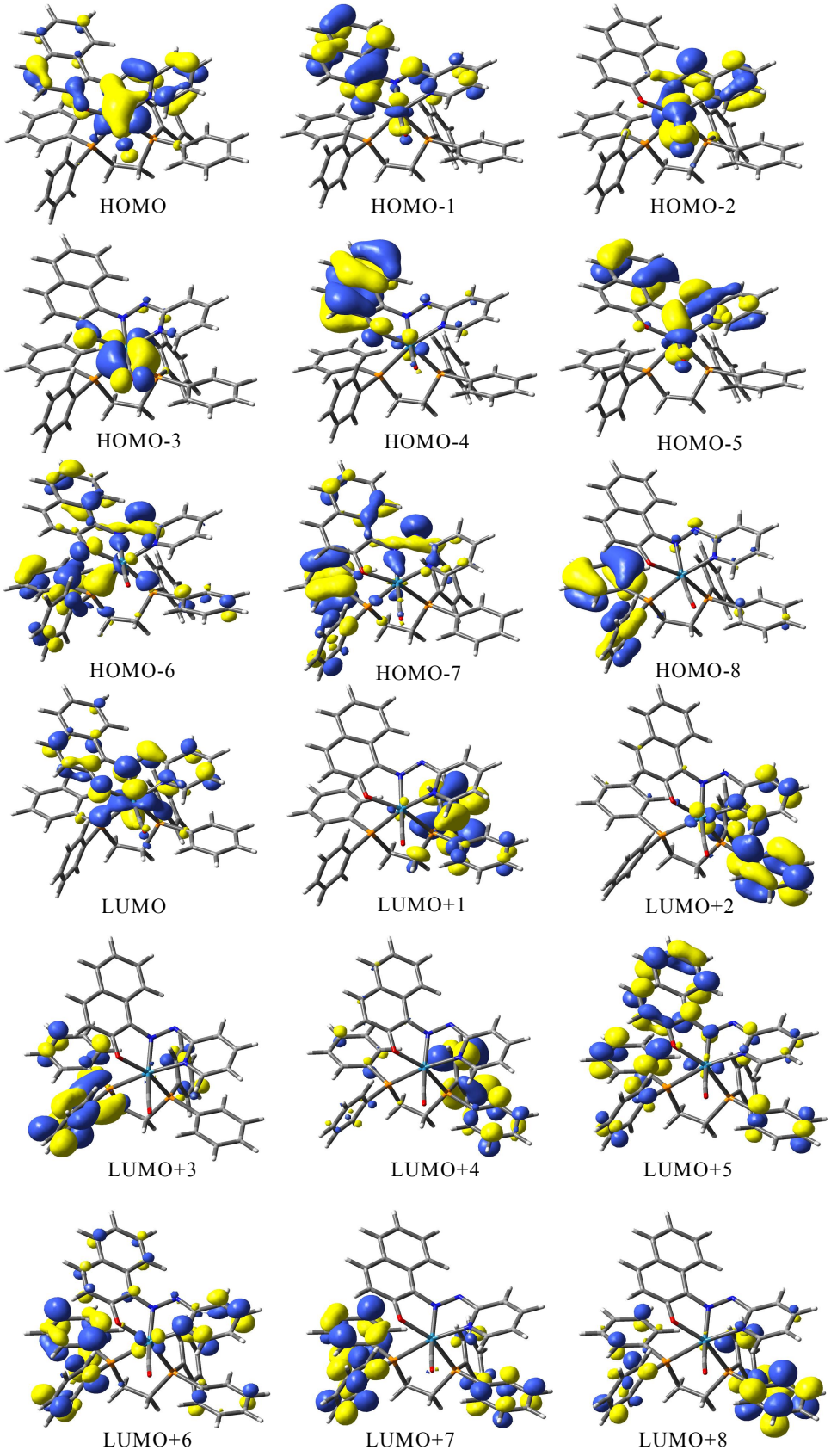

Fig. S2 Isodensity plot of frontier orbitals of [Re(PAN)(CO)(P–P)], **3**.

Table S1 Frontier Molecular Orbital Composition (%) in the Ground State for $[Re_2(PAN)_2(CO)_6]$, **2**.

Orbital	Energy (eV)	Contribution (%)			Main bond type
		Re	CO	PAN	
L+8	-0.851	10.4	36.0	53.6	p(Re)+ π^*(CO)+π^*(PAN)
L+7	-0.906	15.1	44.7	40.1	p(Re)+ π^*(CO)+π^*(PAN)
L+6	-0.976	16.2	45.0	38.8	p(Re)+ π^*(CO)+π^*(PAN)
L+5	-1.181	8.0	23.4	68.6	π^*(CO)+π^*(PAN)
L+4	-1.202	9.1	20.4	70.5	π^*(CO)+π^*(PAN)
L+3	-1.721	3.3	7.0	89.7	π^*(PAN)
L+2	-1.772	3.6	6.7	89.7	π^*(PAN)
L+1	-2.717	3.0	5.5	91.5	π^*(PAN)
L	-2.851	1.3	3.4	95.3	π^*(PAN)
H	-5.687	20.6	10.4	69.0	d(Re)+π(CO)+π(PAN)
H-1	-5.768	20.0	12.0	68.0	d(Re)+π(CO)+π(PAN)
H-2	-6.254	30.7	14.1	55.2	d(Re)+π(CO)+π(PAN)
H-3	-6.274	43.4	21.6	35.0	d(Re)+π(CO)+π(PAN)
H-4	-6.316	53.8	24.7	21.4	d(Re)+π(CO)+π(PAN)
H-5	-6.342	48.1	21.8	30.1	d(Re)+π(CO)+π(PAN)
H-6	-6.663	36.9	15.0	48.1	d(Re)+π(CO)+π(PAN)
H-7	-6.724	37.2	14.0	48.7	d(Re)+π(CO)+π(PAN)
H-8	-6.812	31.2	12.7	56.0	d(Re)+π(CO)+π(PAN)

Table S2 Frontier Molecular Orbital Composition (%) in the Ground State for [Re(PAN)(CO)(P–P)], **3**.

Orbital	Energy (eV)	Contribution (%)				Main bond type
		Re	CO	PAN	(P–P)	
L+8	-0.590	1.6	0.3	6.0	92.1	π^*(P–P)
L+7	-0.633	1.1	0.8	3.5	94.6	π^*(P–P)
L+6	-0.798	4.0	0.2	30.3	65.5	π^*(PAN)+ π^*(P–P)
L+5	-0.832	3.3	0.4	44.0	52.2	π^*(PAN)+ π^*(P–P)
L+4	-0.876	1.1	0.1	6.0	92.8	π^*(P–P)
L+3	-0.946	0.7	0	2.3	97.0	π^*(P–P)
L+2	-1.102	5.5	0.6	24.8	69.1	π^*(PAN)+ π^*(P–P)
L+1	-1.245	1.6	0.4	3.5	94.4	π^*(P–P)
L	-2.042	28.5	1.4	57.5	12.6	p(Re)+ π^*(PAN)+ π^*(P–P)
H	-4.878	37.3	4.7	52.9	5.1	d(Re)+π(PAN)
H-1	-5.264	8.2	1.6	87.6	2.6	π(PAN)
H-2	-5.399	39.2	11.8	41.8	7.1	d(Re)+π(CO)+π(PAN)
H-3	-5.647	69.0	18.5	9.2	3.3	d(Re)+π(CO)
H-4	-6.191	5.0	0.5	92.1	2.3	π(PAN)
H-5	-6.769	15.3	2.7	80.0	2.0	d(Re)+ π(PAN)
H-6	-6.942	5.4	0.8	39.0	54.8	π(PAN)+π(P–P)
H-7	-7.107	3.7	1.1	41.7	53.4	π(PAN)+π(P–P)
H-8	-7.143	0.8	0.4	7.0	91.8	π(P–P)
L+8	-0.590	1.6	0.3	6.0	92.1	π^*(P–P)

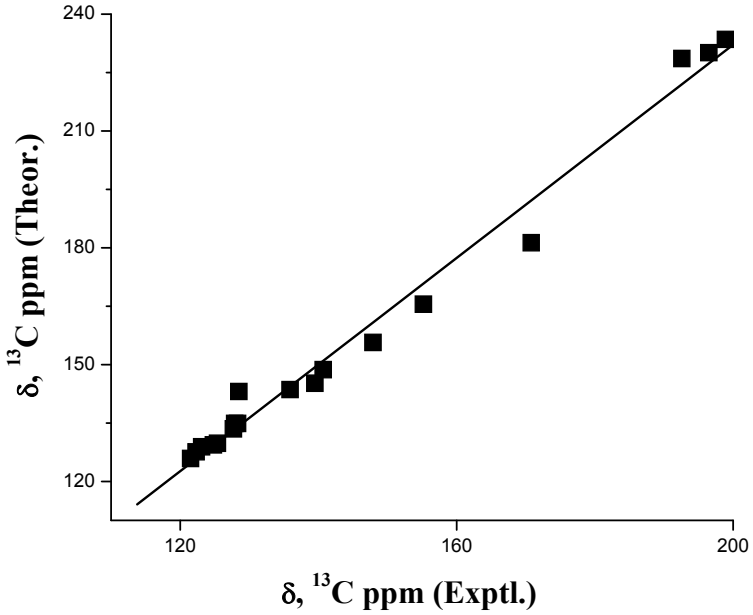

Fig. S3 Linear correlation between the experimental and calculated ^{13}C NMR chemical shifts of $[Re_2(PAN)_2(CO)_6]$, **2**.

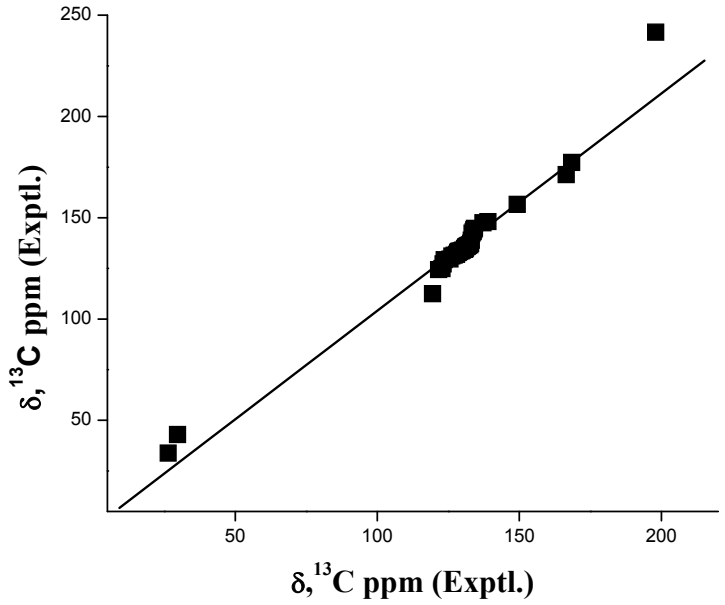

Fig. S4 Linear correlation between the experimental and calculated ^{13}C NMR chemical shifts of [Re(PAN)(CO)(P–P)], **3**.

Table S3 Main calculated optical transition for the complex $[Re_2(PAN)_2(CO)_6]$, **2** with composition in terms of molecular orbital contribution of the transition, Vertical excitation energies, oscillator strength in acetonitrile

Excitation	Composition	E (eV)	Oscillator strength (f)	λ_{theo} (nm)	Assign	λ_{exp} (nm)
1	H-1→ L (100%)	2.4892	0.1749	498.09	MLCT/ LLCT /ILCT	511
2	H→ L+1 (100%)	2.5405	0.0676	488.04	MLCT/ LLCT /ILCT	
3	H-3→ L+1 (23%) H-2→ L (77%)	2.9337	0.5455	422.62	MLCT/ LLCT /ILCT MLCT/ LLCT /ILCT	400
4	H-5→ L+1 (45%) H-4→ L (34%) H-3→ L+1 (20%)	3.1253	0.0190	396.72	MLCT/ LLCT /ILCT MLCT/ LLCT /ILCT MLCT/ LLCT /ILCT	
5	H-9→ L (10%) H-5→ L+1 (14%) H-4→ L (12%) H-3→ L+1 (48%) H-2→ L (16%)	3.1455	0.0791	394.17	MLCT/ LLCT /ILCT MLCT/ LLCT /ILCT MLCT/ LLCT /ILCT MLCT/ LLCT /ILCT MLCT/ LLCT /ILCT	
6	H-11→ L (16%) H-10→ L+1 (12%) H-8→ L+1 (17%) H-7→ L (37%) H-6→ L+1 (17%)	3.3822	0.0567	366.57	MLCT/ILCT ILCT MLCT/ LLCT /ILCT MLCT/ LLCT /ILCT MLCT/ LLCT /ILCT	
7	H-8→ L+1 (21%) H-7→ L (12%) H-1→ L+3 (67%)	3.6494	0.0399	339.74	MLCT/ LLCT /ILCT MLCT/ LLCT /ILCT MLCT/ LLCT /ILCT	313
8	H-11→ L (8%) H-9→ L (28%) H-8→ L+1 (39%) H-6→ L+1 (8%) H-1→ L+3 (16%)	3.6642	0.0144	338.36	MLCT/ILCT MLCT/ LLCT /ILCT MLCT/ LLCT /ILCT MLCT/ LLCT /ILCT MLCT/ LLCT /ILCT	
9	H-5→ L+2 (13%) H-4→ L+3 (11%) H-1→ L+7 (9%) H→ L+5 (44%) H→ L+6 (22%)	3.9517	0.0670	313.75	MLCT/ LLCT /ILCT MLCT/ LLCT /ILCT MLCT/ LLCT /ILCT MLCT/ LLCT /ILCT MLCT/ LLCT /ILCT	
10	H-5→ L+2 (15%) H-4→ L+3 (10%) H-3→ L+2 (9%) H-1→ L+4 (29%) H→ L+5 (19%) H→ L+6 (17%)	4.0725	0.0492	304.45	MLCT/ LLCT /ILCT MLCT/ LLCT /ILCT MLCT/ LLCT /ILCT MLCT/ LLCT /ILCT MLCT/ LLCT /ILCT MLCT/ LLCT /ILCT	
11	H-13→ L (17%) H-12→ L (9%) H-12→ L+1 (11%) H-4→ L+3 (9%) H-3→ L+2 (18%) H-2→ L+3 (11%) H-1→ L+7 (24%)	4.1794	0.0547	296.65	ILCT ILCT ILCT MLCT/ LLCT /ILCT MLCT/ LLCT /ILCT MLCT/ LLCT /ILCT MLCT/ LLCT /ILCT	

Table S4 Main calculated optical transition for the complex [Re(PAN)(CO)(P-P)], **3** with composition in terms of molecular orbital contribution of the transition, Vertical excitation energies, oscillator strength in acetonitrile

Excitation	Composition	E (eV)	Oscillator strength (f)	λ_{theo} (nm)	Assign	λ_{exp} (nm)
1	H-3→ L (13%) H-2→ L (26%) H-1→ L (26%) H→ L (35%)	2.6396	0.2023	469.70	MLCT/LLCT MLCT/ LLCT /ILCT LMCT/ILCT MLCT/ILCT	465
2	H-2→ L (38%) H-1→ L (46%) H→ L+1 (16%)	2.8598	0.2298	433.54	MLCT/ LLCT /ILCT LMCT/ILCT MLCT/ILCT	
3	H→ L+1 (58%) H→ L+3 (27%) H→ L+5 (14%)	3.4318	0.0872	361.28	MLCT/ILCT MLCT/ILCT MLCT/ILCT	366
4	H-4→ L (12%) H→ L+1 (21%) H→ L+2 (15%) H→ L+3 (40%) H→ L+5 (11%)	3.5803	0.1163	346.29	LMCT/ILCT MLCT/ILCT MLCT/ILCT MLCT/ILCT MLCT/ILCT	
5	H-4→ L (22%) H→ L+2 (66%) H→ L+3 (12%)	3.6087	0.0876	343.57	LMCT/ILCT MLCT/ILCT MLCT/ILCT	
6	H-4→ L (51%) H→ L+1 (12%) H→ L+2 (15%) H→ L+4 (12%) H→ L+5 (9%)	3.6586	0.0765	338.88	LMCT/ILCT MLCT/ILCT MLCT/ILCT MLCT/ILCT MLCT/ILCT	
7	H-2→ L+1 (11%) H→ L+4 (46%) H→ L+5 (42%)	3.7684	0.0211	329.01	MLCT/ LLCT /ILCT MLCT/ILCT MLCT/ILCT	

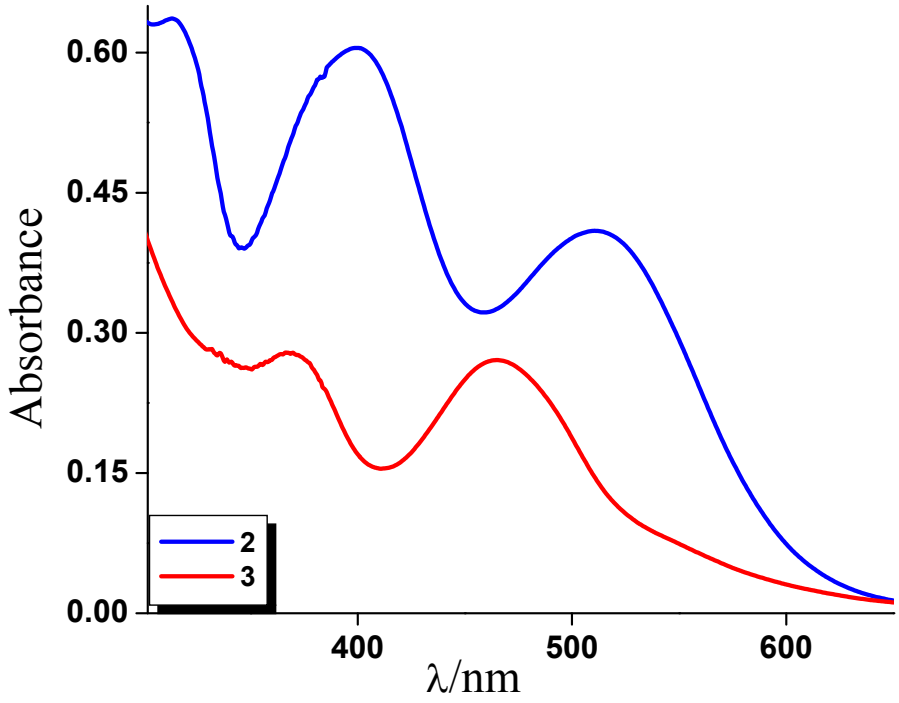

Fig. S5 Experimental absorption spectra of **2** and **3** in acetonitrile media.

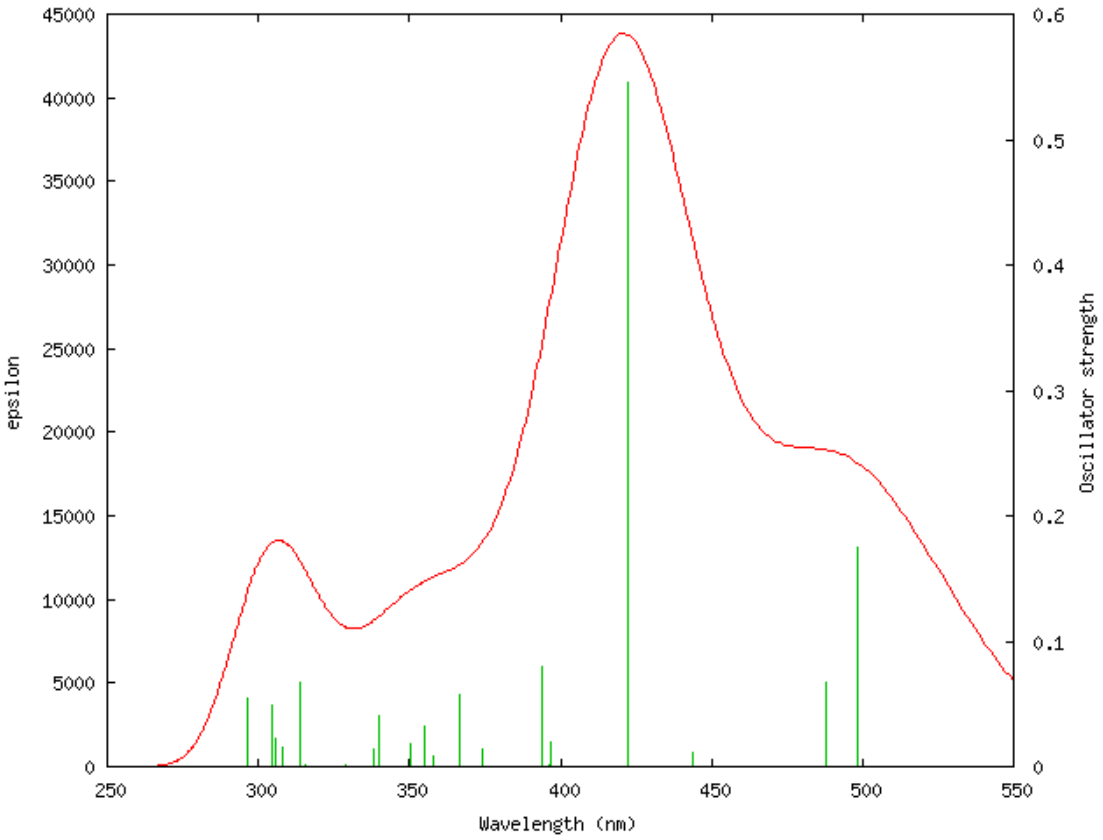

Fig. S6 The simulated absorption spectra of complex $[Re_2(PAN)_2(CO)_6]$, **2** at the TDDFT (B3LYP)/LANL2DZ level in acetonitrile media.

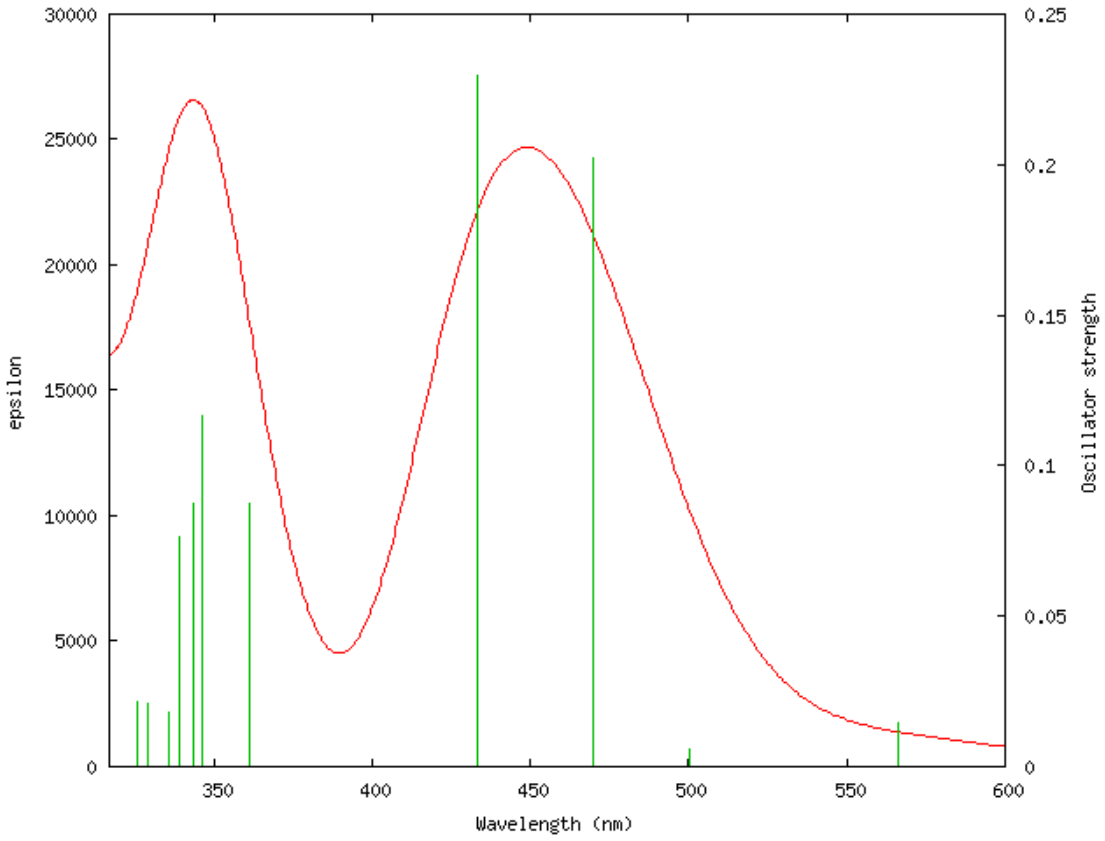

Fig. S7 The simulated absorption spectra of complex [Re(PAN)(CO)(P–P)], **3** at the TDDFT (B3LYP)/LANL2DZ level in acetonitrile media.

Table S5 Frontier Molecular Orbital Compositions (%) in the Excited State for $[Re_2(PAN)_2(CO)_6]$, **2**.

Orbital	Energy (eV)	Contribution (%)			Main bond type
		Re	CO	PAN	
196	-0.853	14.4	66.3	19.2	p(Re)+ π^*(CO)+π^*(PAN)
195	-1.029	9.7	28.0	62.3	π^*(CO)+π^*(PAN)
194	-1.044	12.4	38.4	49.1	p(Re)+ π^*(CO)+π^*(PAN)
193	-1.075	12.3	35.1	52.5	p(Re)+ π^*(CO)+π^*(PAN)
192	-1.203	11.3	30.7	58.0	p(Re)+ π^*(CO)+π^*(PAN)
191	-1.206	8.3	26.7	65.0	π^*(CO)+π^*(PAN)
190	-1.662	3.5	9.6	86.9	π^*(PAN)
189	-1.700	4.2	7.9	87.9	π^*(PAN)
188	-4.229	4.5	4.7	90.8	π(PAN)
187	-4.401	1.7	2.8	95.5	π(PAN)

Table S6 Calculated Triplet Excited State of Complex $[Re_2(PAN)_2(CO)_6]$, **2** in Acetonitrile Based on the Lowest Lying Triplet State Geometry. Main Calculated Vertical Transitions with Compositions in Terms of Molecular Orbital Contribution of the Transition, Vertical Excitation Energies and Oscillator Strength

Excitation	Composition	Energy (eV)	Oscillator Strength (f)	λ_{cal} (nm)	Character	λ_{exp} (nm)
1	189→ 187 (15%)	2.0277	0.0422	611.44	^{3}ILCT	570
	191→ 187 (9%)				^{3}LLCT/^{3}ILCT	
	190→ 188 (75%)				^{3}ILCT	
2	190→ 187 (57%)	2.1235	0.0321	583.88	^{3}ILCT	
	190→ 188 (22%)				^{3}ILCT	
	196→ 188 (21%)				^{3}MLCT/^{3}LLCT/^{3}ILCT	
3	189→ 187 (59%)	2.1846	0.0834	567.54	^{3}ILCT	
	191→ 187 (7%)				^{3}LLCT/^{3}ILCT	
	190→ 188 (10%)				^{3}ILCT	
	192→ 188 (14%)				^{3}MLCT/^{3}LLCT/^{3}ILCT	
	194→ 188 (9%)				^{3}MLCT/^{3}LLCT/^{3}ILCT	
4	189→ 187 (11%)	2.3017	0.0651	538.66	^{3}ILCT	
	193→ 187 (19%)				^{3}MLCT/^{3}LLCT/^{3}ILCT	
	195→ 187 (12%)				^{3}MLCT/^{3}LLCT/^{3}ILCT	
	192→ 188 (48%)				^{3}MLCT/^{3}LLCT/^{3}ILCT	
	194→ 188 (9%)				^{3}MLCT/^{3}LLCT/^{3}ILCT	